



Sulfur dioxide (SO_2) vertical column density measurements by Pandora spectrometer over the Canadian oil sands

Vitali E. Fioletov¹, Chris A. McLinden¹, Alexander Cede^{2,3}, Jonathan Davies¹, Cristian Mihele¹, Stoyka Netcheva¹, Shao-Meng Li¹, and Jason O'Brien¹

¹Environment Canada and Climate Change Canada, Toronto, ON, Canada

²NASA Goddard Space Flight Center, Greenbelt, MD, USA

³LuftBlick, Kreith, Austria

Correspondence to: Vitali E. Fioletov (vitali.fioletov@outlook.com, vitali.fioletov@canada.ca)

Received: 18 February 2016 – Published in Atmos. Meas. Tech. Discuss.: 1 April 2016

Revised: 8 June 2016 – Accepted: 20 June 2016 – Published: 14 July 2016

Abstract. Vertical column densities (VCDs) of SO_2 retrieved by a Pandora spectral sun photometer at Fort McKay, Alberta, Canada, from 2013 to 2015 were analysed. The Fort McKay site is located in the Canadian oil sands region, approximately 20 km north of two major SO_2 sources (up-graders), with total emission of about 45 kt yr^{-1} . Elevated SO_2 VCD values were frequently recorded by the instrument, with the highest values of about 9 Dobson Units (DU; $\text{DU} = 2.69 \times 10^{16} \text{ molecules cm}^{-2}$). Comparisons with collocated in situ measurements demonstrated that there was a very good correlation between VCDs and surface concentrations in some cases, while in other cases, elevated VCDs did not correspond to high surface concentrations, suggesting the plume was above the ground. Elevated VCDs and surface concentrations were observed when the wind direction was from south to southeast, i.e. from the direction of the two local SO_2 sources. The precision of the SO_2 measurements, estimated from parallel measurements by two Pandora instruments at Toronto, is 0.17 DU. The total uncertainty of Pandora SO_2 VCD, estimated using measurements when the wind direction was away from the sources, is less than 0.26 DU (1σ). Comparisons with integrated SO_2 profiles from concurrent aircraft measurements support these estimates.

1 Introduction

Sulfur dioxide (SO_2) plays an important role in Earth's atmospheric chemistry and climate. It forms sulfate aerosols that

influence weather and climate and leads to acid deposition through the formation of sulfuric acid (H_2SO_4) (Hutchinson and Whitby, 1977). It is also a designated criteria air pollutant in many countries that poses a direct hazard to public health (Longo et al., 2010; Pope and Dockery, 2006). Active volcanoes are the primary natural source of SO_2 , while coal-burning power plants, smelters, and oil refineries are the primary anthropogenic emitters of SO_2 into the atmosphere. In Canada, the majority of SO_2 emissions come from three sources: 32 % from smelting and refining for non-ferrous metals, 22 % from coal-fired electricity generation, and 21 % from the petroleum industry (Wood, 2012). One of the largest sources of atmospheric pollutants, including SO_2 , in Canada is the oil sands operations. Located in the province of Alberta, the oil sands contain vast deposits of bitumen oil mixed with sand, clay, and water. Environmental and health concerns associated with the oil sands operations, including air quality and acid deposition, are well known (Kelly et al., 2010). Highly elevated levels of SO_2 over the oil sands area have been detected there (Simpson et al., 2010) and are a subject of concern. Due to the large size of the oil sands operation area, satellite measurements are an appealing approach for air pollution monitoring in this region.

The applications of satellites for monitoring SO_2 have been progressing rapidly during the last 2 decades. They are widely used to monitor volcanic (Carn et al., 2003, 2013; Fioletov et al., 2013; Krueger et al., 2000; Rix et al., 2012; Theys et al., 2013) and anthropogenic sources (Carn et al., 2007; Clarisse et al., 2011; Eisinger and Burrows, 1998; Fioletov et al., 2011, 2013; de Foy et al., 2009; Georgoulias

et al., 2009; Lee et al., 2011; Nowlan et al., 2011; Thomas et al., 2005, Krotkov et al., 2016). More recently, satellites have been used for monitoring SO_2 (and NO_2) emissions and trends in the oil sands region (McLinden et al., 2015, 2012, 2014). Many satellite instruments provide vertical column densities (VCDs) once a day, but derivation of surface concentrations from them is not straightforward (Knepp et al., 2015). Time-resolved ground-based measurements of the same quantity, VCD, help both in the validation of satellite measurements and the facilitation of a better interpretation of satellite data and their links to surface concentration (Richter et al., 2013).

Ground-based observations of SO_2 VCDs were first made by Brewer spectrophotometers, using the strong absorption features of SO_2 in the ultraviolet (UV) part of the spectrum (Kerr et al., 1988). The Brewer spectrophotometer operating in the direct-sun (DS) mode measures UV at five wavelengths between 306 and 320 nm to retrieve column ozone and SO_2 . Such measurements have been used to monitor volcanic SO_2 (Krueger et al., 1995) and anthropogenic SO_2 in extreme pollution events (De Backer and Muer, 1991; Zerefos et al., 2000). The uncertainty of the Brewer DS SO_2 measurements is about 1–2 Dobson Units (DU, where 1 DU is equal to 2.69×10^{16} molecules cm^{-2}) and is typically insufficient for air quality applications. A Brewer spectrometer can also measure global spectral UV irradiance on a horizontal surface in the spectral range 290–325 or 286–363 nm (depending on the type) with a 0.5 nm increment. Pronounced SO_2 absorption features were seen in these global UV spectra when SO_2 amounts were high (Bais et al., 1993). SO_2 VCD can be even derived from such global spectral UV measurements (Fioletov et al., 1998). However this method of SO_2 VCD retrieval is less sensitive than the Brewer DS method and has the detection limit of about 5 DU. A more accurate method (with an uncertainty as low as 0.13 DU) based on Brewer “group-scan” spectral direct-sun radiation measurements at 45 wavelengths from 306 to 324 nm was developed (Kerr, 2002), but not widely implemented due to its complexity.

The ground-based multi-axis differential optical absorption spectroscopy (MAX-DOAS) method is another technique used for ground-based SO_2 retrievals. The method is based on scattered sunlight measured in the UV part of the spectrum at different elevation angles with data analysed using the DOAS technique (Platt and Stutz, 2008). In addition to total VCD, the method can provide some information on the vertical profile. It was widely used for measurements of volcanic SO_2 under the Network for Observation of Volcanic and Atmospheric Change (NOVAC) project (Galle et al., 2010). Only a few studies have focused on MAX-DOAS measurements of anthropogenic SO_2 (Wang et al., 2014; Wu et al., 2013; Theys et al., 2015). The uncertainty of the retrieved SO_2 estimated from the spectral fitting error is about 0.1 DU (Wang et al., 2014).

Pandora (SciGlob, <http://www.sciglob.com/>) is a recently developed instrument for UV and visible spectral measurements, which was primarily designed for direct-sun observations, but is also capable of conducting zenith sky (ZS) and MAX-DOAS measurements. Similar to the Brewer instrument, it tracks the sun, but as it measures the entire spectrum at once, a DOAS-type algorithm can be applied. The instruments were used in several NASA Deriving Information on Surface Conditions from Column and Vertically Resolved Observations Relevant to Air Quality (DISCOVER-AQ) campaigns. DISCOVER-AQ is a series of field missions with an overarching objective to improve the interpretation of satellite observations to diagnose near-surface conditions relating to air quality (Reed et al., 2015). It has been demonstrated that Pandora can successfully measure total column ozone and NO_2 (Herman et al., 2009, 2015; Tzortziou et al., 2012, 2015). The instrument characteristics are suitable for total column SO_2 measurements, but available information on Pandora SO_2 measurements is very limited (Knepp et al., 2015). This is probably a result of most Pandora instruments being deployed away from major SO_2 sources. In 2013, a Pandora instrument, along with other instrumentation, was deployed to the oil sands region where relatively high SO_2 column amounts are common (McLinden et al., 2012; Simpson et al., 2010). This made it possible to establish optimal retrieval procedures for the Pandora SO_2 measurements, estimate uncertainties, and study the relationship between total columns and surface concentrations.

2 Instruments and locations

The Pandora spectrometer system is based on an Avantes symmetric Czerny-Turner optical bench design with a 2048 CCD linear array detector. The Pandora spectrometer system consists of an optical head sensor, mounted on a computer controlled sun-tracker and sky-scanner, and connected to an Avantes array spectrometer by means of a 400-micron core diameter single strand multi-mode optical fibre. It operates in the 280–530 nm spectral range with a 0.6 nm slit function width (full width at half maximum). A detailed description of the instrument is given by Herman et al. (2009). Wavelength calibration and slit functions for Pandora instruments were determined by the manufacturer from lamp emission lines (Hg, Cd, Cu, In, Mg, Zn). Wavelength stability is validated during instrument operation by an analysis of the solar Fraunhofer line structures. Stray light in the 304 to 330 nm range (used for SO_2 retrievals) is reduced by utilizing a U340 (280–380 nm) band pass filter with a cut-off limit at 380 nm. Further stray light correction by the Pandora processing software is obtained from pixels corresponding to 280 to 285 nm, which contain almost zero direct illumination. We used the instrument in DS and ZS modes but will limit this study to DS measurements only. To allow for the detection of different absorbers, the instrument periodically measures UV

spectra with the U340 filter on and off, with an interval of about 90 s.

In 2013, Environment Canada (EC) acquired two Pandora sun spectrometers from SciGlob. One of them, with Serial Number 104, after a 3-week testing period at Toronto, was deployed to Fort McKay (57.184°N , 111.64°W) in the oil sands region, where it began operations on 15 August 2013. The instrument head was mounted on a tripod, and the spectrometer and computer were installed in waterproof plastic housing (Fig. 1, left). The head and the housing were connected by 10 m long optical, data, and power cables. Such configuration provided a rapid deployment of the instrument, but it could not withstand a cold Alberta winter. The instrument was shipped back to Toronto on 3 December 2013. It was then redeployed on 21 August 2014 in a different configuration with the instrument head installed on the roof of the EC instrument trailer, while the spectrometer and computer were installed inside the trailer in a temperature-controlled environment (Fig. 1, right).

The site at Fort McKay is equipped with various instruments for air quality measurements. In this study, we used the in situ measurements of SO_2 as well as the wind speed and direction data provided by Recordum Airpointer[®] suite of instruments (<http://recordum.eu/recordum-airpointer/>). According to the manufacturer, the precision of SO_2 measurements is about 1 ppb. The Airpointer reports data with a 1 min time resolution. We used 10 min averages matched with 10 min averaged Pandora data.

Fort McKay is a small town (population of 600) surrounded by five oil sands surface mining facilities to the north and south. There are two major SO_2 sources located south of Fort McKay: the Syncrude Mildred Lake plant is located 16 km to the south of Fort McKay and the Suncor Millenium Plant 23 km south-south-east. According to the National Pollutant Release Inventory (NPRI, <http://www.ec.gc.ca/inrp-npri>), the 2014 annual emissions were about 26 and 17 kt of SO_2 per year from the Syncrude and Suncor facilities, respectively. There is also a source (Horizon Oil Sands processing plant and mine) 18 km north, but the emission from that source are 4 kt per year. There are hundreds of kilometres of pristine boreal forests to the west and east from Fort McKay with no SO_2 sources. Thus, the pollution level at Fort McKay is largely dependent on the wind direction.

Another Pandora instrument (S/N 103) was installed on 14 October, 2013 on the roof of the EC building at Downsview (43.782°N , 79.47°W), a typical urban location in Toronto. The instrument head was mounted on a tripod, but the spectrometer and computer were located inside the building and connected to the head by a 10 m cables. The same configuration was used for Pandora 104 when the instrument was in Toronto. The two instruments were run side-by-side from January to June 2014, making a direct comparison possible. According to NPRI, there are no large SO_2 emission point sources in the vicinity of the EC building in Toronto, but there are multiple sources with emissions under 10 kt per



Figure 1. Pandora instruments at Fort McKay in (left) 2013 and (right) 2014–2015. In 2013, the instrument's optical head was installed on a white Brewer tripod and the spectrometer and computer were inside the black box to the right. From 2014, the head was installed on the roof of a trailer with the spectrometer and computer located inside the trailer.

year in the area. The largest source with total emissions of about 12 kt per year is a cluster of plants on the west coast of Lake Ontario, about 60 km from the site.

3 Pandora's SO_2 algorithm and data

The Pandora Operation and Analysis Software Suite (Version 1.6, available from <http://avdc.gsfc.nasa.gov/pub/tools/Pandora/install/>) was used for data processing and retrieval. The software can be configured to include a specific set of retrieved species and to use an extraterrestrial reference spectrum. The information about the retrieval algorithm and configuration settings is available from the software manual. In particular, the software allows for the selection of a spectral fitting window. MAX-DOAS retrievals tend to use narrow spectral windows to avoid differences in the air mass factors (μ) for individual wavelengths within the window caused by differences in optical paths due to scattering. This factor is far less important for DS measurements.

The first step in the Pandora spectral fitting algorithm is to subtract the irradiance logarithm of the measured spectra from the irradiance logarithm of the reference spectrum. Then, a simultaneous least-squares fit is applied to the difference between measured and reference spectra (see Herman et al., 2009 for details) as illustrated by Fig. 2. The fitted functions are a low-order polynomial, the absorption spectra of SO_2 , ozone, and other atmospheric absorbers, and wavelength shift and squeeze functions.

The Pandora standard algorithm uses a SO_2 absorption cross section at 295 K (Vandaele et al., 1994) in the retrieval. As the SO_2 absorption cross section possesses very distinct absorption features (Fig. 3a), a wider fitting window, including more spectral lines, should reduce the uncertainties of the retrievals. Figure 3 also shows SO_2 values retrieved for the 304–311, 311–330, 304–330, and 306–330 nm spectral windows based on measurements taken at Fort McKay on 14 September 2013 (Fig. 3c), and at Downsview on 16 March 2014 for both instruments (Fig. 3b and d). It is evident from

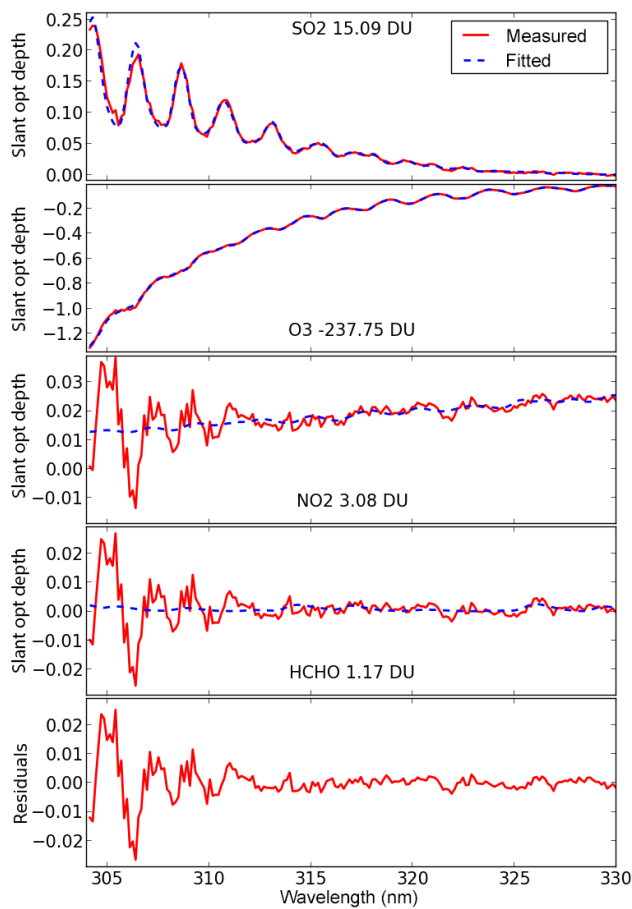


Figure 2. Fitted Pandora slant column optical depths (blue) for a measurement at Fort McKay on 2 August 2015 at 07:42 MST (red) when some of the highest SO_2 values were observed. The synthetic reference spectrum was used in the fitting (see text for details). The negative O_3 slant column means that there was more O_3 in the reference than in the measurements at 07:42 MST. Note that NO_2 and HCHO are fitted in this fitting windows, but only to improve the results for SO_2 . The measured (red) lines for each gas were obtained from the measured irradiance logarithm by subtracting all other fitting functions except the absorption spectrum-based fit for that gas.

the plot that the first two windows produce SO_2 values that have a much larger scattering than the values retrieved based on the entire 304–330 nm spectral window. The SO_2 absorption spectrum has strong peaks in the 304–311 nm spectral window, but the absolute signal is weaker and the stray light is higher than in the 311–330 nm spectral window. However the weaker SO_2 absorption features in 311–330 nm result in increased sensitivity to the influence of ozone and possibly other absorbers.

The 306–330 nm spectral window was used in this study. When SO_2 is high, the values retrieved using all four spectral windows are very similar. The retrievals using the 306–330 nm spectral window are nearly identical to those obtained for the 304–330 nm window, but produce slightly

lower uncertainties. The software also has the option to use a prescribed extraterrestrial spectrum or to generate it from the measurements (“synthetic reference spectrum”). Both options were tested and the latter option was used as it produces slightly smaller uncertainties. The synthetic reference spectrum is derived from an average of the logarithms of about 100 low integration time spectra measured near noon in Toronto. Then, the slant column amount for each trace gas in this spectrum was estimated and added to the spectrum to get an “absorption-free” reference spectrum (see Herman et al., 2009 for details). Note that the synthetic reference spectrum was established from clear sky measurements in Toronto before each instrument deployment to Fort McKay and then used to process all subsequent data. SO_2 VCDs at Toronto are low, so the synthetic reference spectrum is close to an SO_2 absorption-free reference spectrum. The calibration procedure discussed below removes any biases caused by remaining SO_2 signals in the reference spectrum.

Several criteria were used for data filtering. The instrument integration time varies from 4 to 4000 ms depending on the signal strength. To exclude measurements when the sun was covered by clouds, a 500 ms cut-off limit was used as a quality control tool: measurements that required more than 500 ms integration time were rejected. Furthermore, for high sun elevations, lower cut-off limits were used: 300 ms for air mass (μ) value $\mu < 3$ and 100 ms for $\mu < 2$. Measurements taken at $\mu > 5$ were not used. In addition to SO_2 vertical column calculation, the Pandora data processing software calculates its statistical uncertainty. After the filtration by the integration time, the statistical fitting uncertainties are less than 0.05 DU for 60 %, and between 0.05 and 0.15 DU for about 30 % of all retrieved VCD values. The remaining 10 % have higher uncertainties and are related to measurements at low sun position or under very thin clouds, but some of them can still be useful. Only data with a fitting uncertainty of SO_2 VCD < 0.35 DU were used.

All data were processed with the both reference spectra and with several spectral windows. Then all retrieved SO_2 values for each measurement were compared. We encountered one practical problem related to the fitting algorithm that appears when the SO_2 amount is close to zero and the measurements are relatively noisy (e.g. due to thin clouds). In general, the 306–330 nm spectral window and the synthetic spectrum give the best results, but on some occasions, that fitting algorithm finds the best fit with a small wavelength offset and an artificially elevated SO_2 value (by as much as 1 DU compared to the values for the other reference spectrum or for the same spectrum, but different fitting windows). Only 2–3 % of the data are affected by this error, but they are very noticeable on time series plots. A simple filtering by the standard error of retrieved SO_2 (< 0.2 DU) and/or by the wavelength offset removes these erroneous data, but it can also remove some valid observations. As mentioned, there are two options for the reference spectrum: an independently measured extraterrestrial spectrum (“prescribed refer-

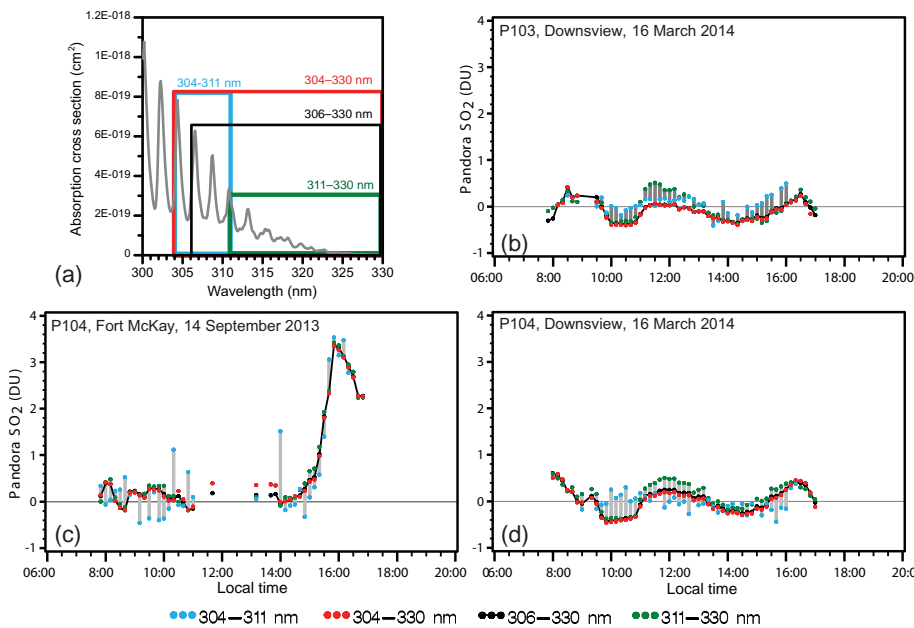


Figure 3. Examples of SO_2 VCD retrieved using different spectral windows as indicated on the plot. Data from Pandora 104 at Fort McKay, 14 September 2013, and Downsview, 16 March 2014, are shown. Different colours represent different spectral windows used for the fitting. Grey bars connect SO_2 values retrieved from 304–311 and 311–330 nm spectral windows.

ence spectrum") or generated from the measurements themselves ("synthetic reference spectrum"). Such problematic cases were processed with the prescribed spectrum that appear to give better results in this situation than processing with the synthetic reference spectrum used for all other retrievals.

The calibration procedure for NO_2 DS DOAS measurements (determining the absolute slant column amount in the reference spectrum) is described by Herman et al. (2009). It is based on a linear fit of the lowest 2 % (or so) slant column values as a function of the air mass. Unlike NO_2 measurements with a precision of 0.01 DU (Herman et al., 2009), retrievals of SO_2 have to deal with relatively high noise in individual measurements, their precision is about 0.17 DU (shown later). This means that the 2nd percentile will be determined largely by the noise and not the lowest VCD values. Additionally, unlike stratospheric NO_2 that is always present in any NO_2 VCD retrieval, we can assume that there is a certain fraction of measurements without any measurable SO_2 presence in the atmosphere. We modified the NO_2 calibration approach to make it more suitable for SO_2 by considering higher percentiles and then adjusting the "baseline" level using known characteristics of the noise distribution function as described below.

Figure 4 (top) shows slant column SO_2 measured at Fort McKay in August–September 2013 as a function of the air mass factor μ . In the absence of any SO_2 , the slant column values should be scattered around the zero line, so the mean and median values as a function μ of should be equal to zero. If, however, the reference spectrum is not absolutely correct,

it may contain structures that the fitting procedure interprets as a contribution from SO_2 absorption. Similarly, if the ozone absorption is not accounted for completely, the fitting procedure could produce a residual SO_2 signal that depends on μ . Thus, even in the case with no SO_2 in the atmosphere, the mean (or median) values of slant column are not constant, but can be described as a linear function (in the simplest case) of μ . That function could be used as a reference corresponding to zero SO_2 slant column values in the SO_2 -free atmosphere. If we assume that the noise is Gaussian with a known standard deviation, then the mean can be also calculated from any percentile value because the Gaussian distribution is determined by only two parameters. This can be used to determine the "no SO_2 " atmosphere mean value in the case of real atmosphere.

If we assume that SO_2 is present even in a fraction of all observations at an otherwise SO_2 -free site, then the mean value will be elevated compared to the SO_2 -free "clean" atmosphere and therefore it cannot be used as a reference in the calibration procedure. However, the low percentiles (e.g. 5th, 10th, or 25th) of slant column values are close to the same percentiles for clean conditions as they correspond to conditions with no SO_2 in the atmosphere (e.g. when the wind is from the west where there is no sources). This makes them suitable for determining the absolute slant column amount in the reference spectrum as the mean value for the no SO_2 atmosphere. There are two potential complications: first, the low percentiles could be biased low relative to zero SO_2 conditions due to random errors, thereby resulting in scattering of data points. The lower the percentile value, the larger

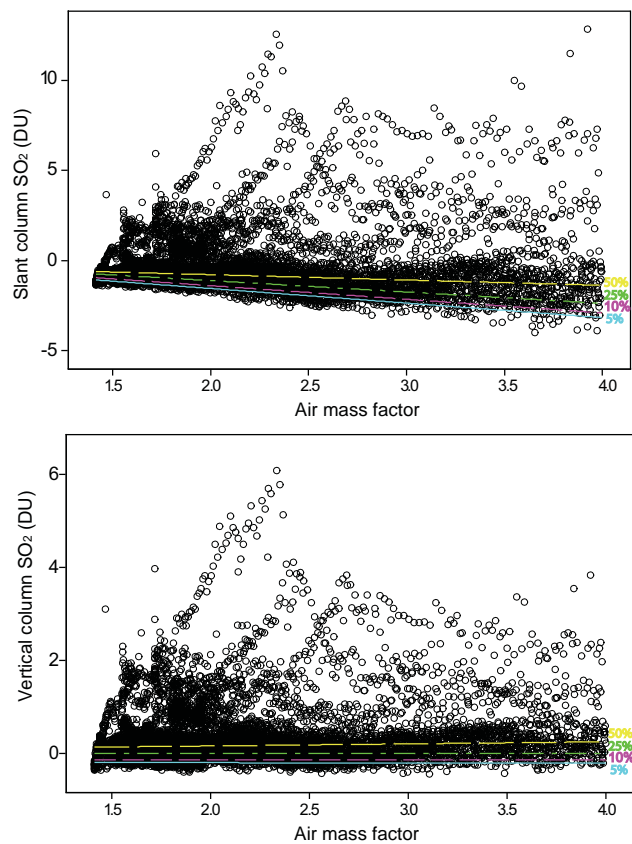


Figure 4. Top: slant column densities derived from 306 to 330 nm spectral fitting of Pandora 103 data at Fort McKay in August 2013. Bottom: vertical column densities derived from the same data using the fit based on 25th percentile (see text for details). The data were grouped into 10 min bins and only bins with between five and seven individual measurements were used for the comparison. The total number of bins was 1844. The correlation coefficient between the plotted data is 0.7.

that bias. Second, the standard deviation of the scattering increases with the air mass factor as the signal strength declines, resulting in higher errors and lower values in the low percentiles.

The intercept (a) and slope (b) of different percentile lines were determined by a method that is based on quintile regressions (Koenker and Bassett, 1978). Once the slope and intercept of the reference line are known, the VCD values can be derived from slant column density (SCD) as $\text{VCD} = (\text{SCD} - a)/\mu - b$. This selection of a particular percentile line as a reference introduces a bias that can be corrected using the information about measurement uncertainties as discussed below. We used the 25th percentile in our calculations. Note that the slopes of the percentile lines are very similar, and the difference between the 25th percentile intercept and 50th or 10th percentiles intercepts for VCDs is +0.16 and -0.12 DU respectively.

The fact that the slope of the regression line for the SCD vs. μ in the absence of SO_2 is negative may seem counterintuitive, but the spectral fitting procedure is dominated by the ozone signal. A small imperfection in accounting for ozone

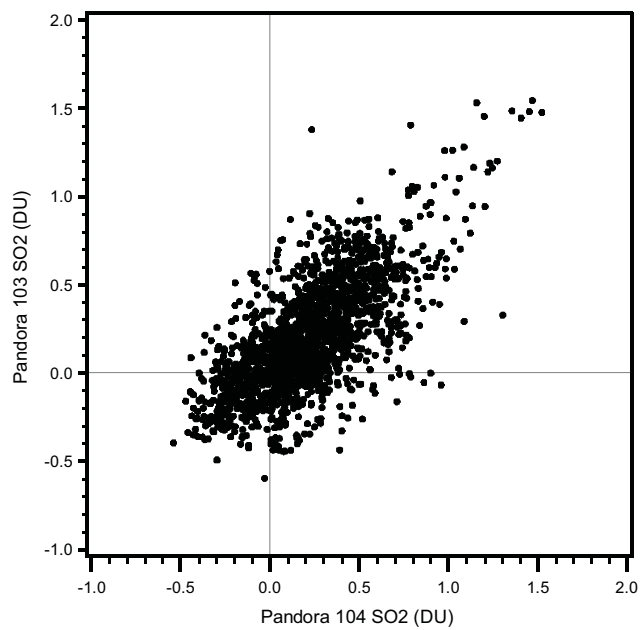


Figure 5. The scatter plot of coincidental SO_2 measurements at Downview by Pandora 103 and 104 in January–July 2014. The data were grouped into 10 min bins and only bins with between five and seven individual measurements were used for the comparison. The total number of bins was 1844. The correlation coefficient between the plotted data is 0.7.

absorption can be compensated by a biased SO_2 signal. As the shape of the ozone profile and the temperature of the ozone layer change throughout the year, this calibration procedure was applied on a monthly basis. The correction to the VCD (that is equal to $-a/\mu - b$) introduced by this calibration procedure is not negligible and changes throughout the year. For $\mu = 3$, the correction value ranges from -0.15 DU in October to 0.55 DU in May.

Estimation of the instrument precision would be an easy task if we could install the instrument in an SO_2 -free location, but this was not the case for our sites. However, the side-by-side operation of two instruments at Toronto made it possible to study the precision of Pandora's SO_2 measurements. Figure 5 shows a scatter plot of the SO_2 values by the two instruments from 16 January 2014 to 31 July 2014 when both instruments were at the Downview site. Typically, the SO_2 VCD values in Toronto are relatively small, less than 1.7 DU. The correlation coefficient between the measurements of the two instruments shown in Fig. 5 is 0.7. Using Grubbs estimation method (see Appendix A for details) and assuming that there is no multiplicative bias between measurements, we can calculate that the standard deviations of instrument errors are 0.18 and 0.16 DU for Pandora 103 and 104 respectively.

This information about the instrument errors can be used to reduce the effect of an arbitrary selection of the percentile line as a reference used by the calibration procedure. If we assume that the instrumental errors have a Gaussian distribu-

tion with a 0.17 DU standard deviation, then in the absence of any SO_2 , the 25th and 10th percentile values would be -0.11 and -0.22 DU respectively. These values represent the biases introduced by the calibration procedure and should be added back to the retrieved values. Note that the lower the percentile value, the less the calibration procedure is affected by non-zero SO_2 values. However, the lower the percentile value, the higher the uncertainty of the percentile estimate and the higher the impact of the uncertainty of the instrumental error estimate can have on the size of the bias. In our case, either the 25th or 10th percentile seems to be optimal. As the distance between them from the Gaussian distribution with $\sigma = 0.17$ DU is -0.11 DU, very close to the -0.12 DU value from the Fig. 4 (bottom) estimates, there is no impact on the results regardless of what percentile value to use.

The precision of Pandora instruments is high and the two instruments track each other reasonably well, but there could be systematic errors related to the retrieval algorithm itself. Figure 3b and d show an extreme example when both instruments reported fluctuations around the zero line with negative values as low as -0.4 DU. The spectral fitting algorithm includes ozone absorption spectrum as one of the main fitted functions. The ozone optical depth is about 2 orders of magnitude higher than the SO_2 optical depth (for 1DU of SO_2 and the 311–330 nm spectral window). Even a small imperfection in accounting for ozone absorption could cause a substantial error in retrieved SO_2 . Column ozone was high on that day (420 DU) and the incomplete removal of ozone absorption features by the spectral fitting algorithm could be a possible explanation for such a large negative value. The SO_2 values retrieved using the 304–311 nm spectral window, where the influence of other absorbers is smaller due to the stronger SO_2 absorbing features, are close to the zero line. Similar fluctuations with positive and negative values at Fort McKay were observed on days when surface concentrations were close to zero with the site at upwind of the sources, indicating these fluctuations were not related to real changes in SO_2 VCD. Further improvement of the retrieval algorithm could increase the accuracy of Pandora's SO_2 measurements.

4 SO_2 measurements at Fort McKay

The site at Fort McKay is located 20 km from the major emission sources and SO_2 values as high as 9 DU are observed from time to time. Time series of SO_2 measurements at Fort McKay in August 2013–October 2015 are shown in Fig. 6. Different colours and symbols represent different uncertainties of the retrieved values as estimated by the Pandora processing software.

The first days of the Pandora operation at Fort McKay revealed that a combination of strong emissions from the industrial sources to the south with southern winds result in “pollution events” characterized with high VCD values of SO_2 and NO_2 . An example of such an event on 23 August

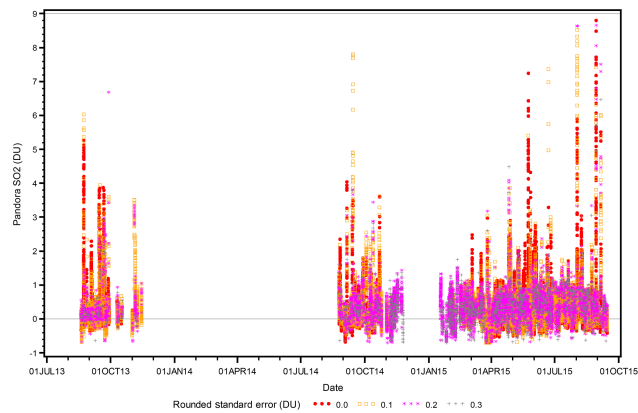


Figure 6. Time series of SO_2 measurements at Fort McKay from August 2013 to October 2015. Different symbols and colours represent different standard errors estimated by the fitting algorithm. Data from December 2014–January 2015 are missing because of low sun elevation ($\mu > 5$).

2013 is shown in Fig. 7a. During that event, the wind direction was from the south or southeast, i.e. from the direction of the major pollution sources.

Although the VCD and surface concentration are different qualities, they are often affected by the same plume and therefore correlated. In situ measurements on 23 August 2013 demonstrated the same behaviour of surface SO_2 and VCDs as illustrated by Fig. 7a, with a relationship where each 10 ppbv at the surface corresponds to about 1 DU in total column. However, this column–surface relationship is different from event to event. Figure 7b and c show examples of pollution events on 4 and 5 November 2013, when 1 DU corresponds to about 5 and 20 ppbv respectively. On some occasions, the VCD and surface concentration show a similar behaviour for many hours (Fig. 7d), while on other days the changes in surface concentration follow the VCD changes with some time lag (Fig. 7e), probably due to the shape of the plume, or do not really show any good correlation (Fig. 7f). In the case of 2 August 2015 (Fig. 7f), the SO_2 plume was probably above the ground early in the morning and was not detected by in situ instruments.

High surface concentrations should contribute to elevated vertical columns. The examples presented above indicate that the opposite may not be always true: elevated vertical column densities may be related to plumes that are above the ground and therefore may not produce high surface concentrations. This is further illustrated by Fig. 8 where scatter plots of surface concentrations binned by VCD values and VCDs binned by surface concentrations are shown.

Surface wind data were used to study the dependence of VCDs and surface concentrations on wind directions. The main SO_2 emission sources are located within about 20 km to the south of Fort McKay, and the winds from the south generally produce elevated SO_2 values. Figure 9a confirms that

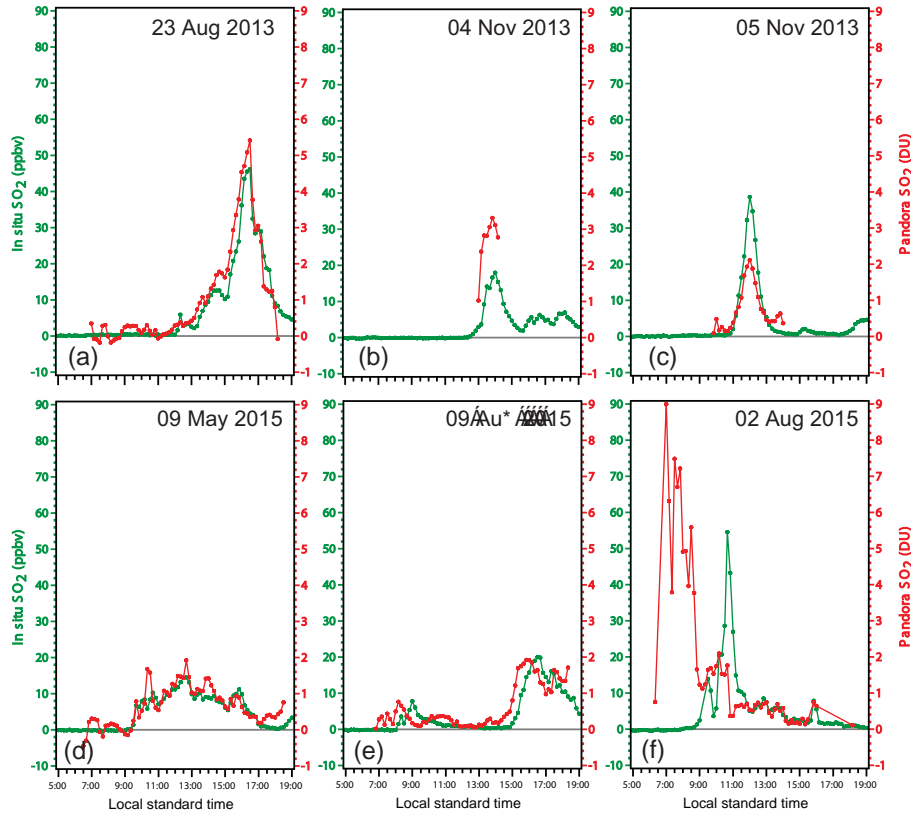


Figure 7. Vertical column density (DU) measured by the Pandora spectrometer at Fort McKay and in situ SO_2 concentration (ppbv) measured at the same location for 6 days, which illustrate fluctuations of VCDs and surface concentrations. Note that the vertical scales are the same for all six plots.

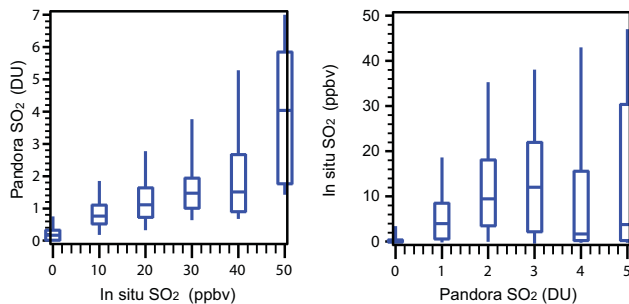


Figure 8. VCD and surface concentration SO_2 data binned by (left) surface concentration and (right) VCD values. Binned VCD and surface concentration data show a clear link between the two parameters, but binning by Pandora's values gives a different result from the binning by in situ data. When the surface concentration is elevated, vertical columns are also elevated. However, in about 25 % cases, surface concentrations are close to zero even when the vertical column values are elevated. The bottom and top edges of the box are located at the sample 25th and 75th percentiles; the whiskers correspond to the 5th and 95th percentiles. The centre horizontal line is drawn at the median.

surface SO_2 concentrations are the highest when the wind direction is south-southeasterly. This can be seen for both the mean values and for extremes (90th percentile).

As discussed in Sect. 3, the calibration procedure is based on the assumption that a certain fraction of all measurements corresponds to clean conditions. As Fig. 9a shows, surface concentrations are very low for most wind directions except south and south-east. This can be used to refine the calibration-related bias in Pandora data mentioned in Sect. 3. A minimum in SO_2 of about zero was found for winds from the west as expected from the location of industrial sources. We can assume that this direction represents clean conditions and this gives us an additional confidence in the suggested calibration procedure. Figure 9b shows Pandora SO_2 VCD as a function of the wind direction with this bias removed. As expected, it is very similar to the distribution of surface concentrations from Fig. 9a.

It should be noted that the 90th percentile values for the direction from west are 0.25–0.3 DU (Fig. 9b). This can be interpreted as yet another estimate of the overall uncertainty of Pandora's SO_2 data. If we assume the Gaussian distribution of the errors, then the 0.3 DU value of the 90th percentile corresponds to 0.23 DU value of the standard deviation. The standard deviation as calculated directly is between 0.22 and

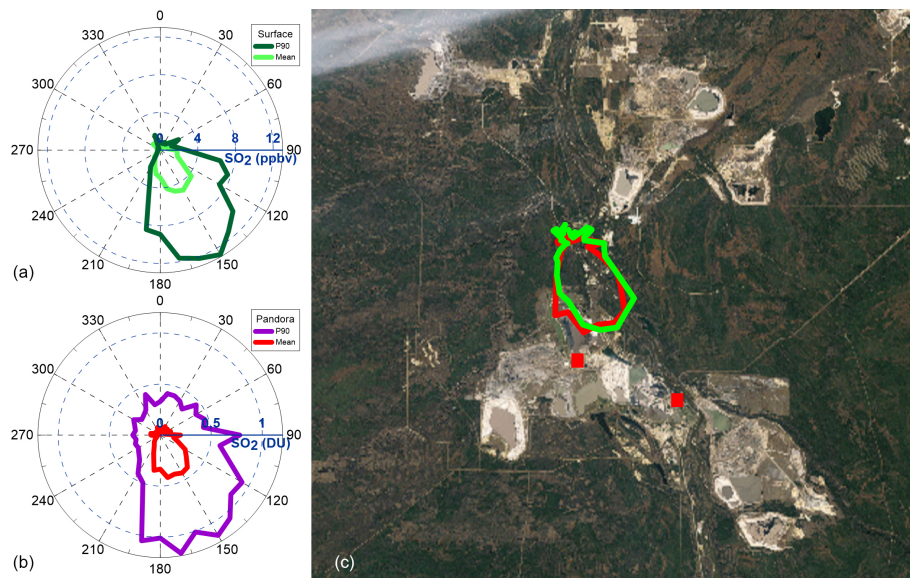


Figure 9. The mean and 90th percentile of in situ SO_2 concentration (a) and Pandora SO_2 VCD (b) at Fort McKay as a function of the wind direction in 2013–2015. Both Pandora and in situ data show similar patterns: high SO_2 values are associated with south-east winds (c). The mean values from the plots (a) and (b) are overlaid with Landsat images of the surface mining area (<http://earthobservatory.nasa.gov/Features/WorldOfChange/athabasca.php?all=y>). The plots are based on simultaneous Pandora and in situ measurements averaged over 10 min intervals. The 0, 90, 180, and 270° azimuths correspond to the northern, eastern, southern, and western wind directions respectively. The two red squares indicate the major SO_2 emission sources. Data for this plot were binned into 10° bins by the wind direction.

0.26 DU for six 10° bins corresponding to clean western directions. These values are higher than the previously estimated 0.17 DU value of the instrument precision, but they also include the errors related to imperfection of the retrieval algorithm.

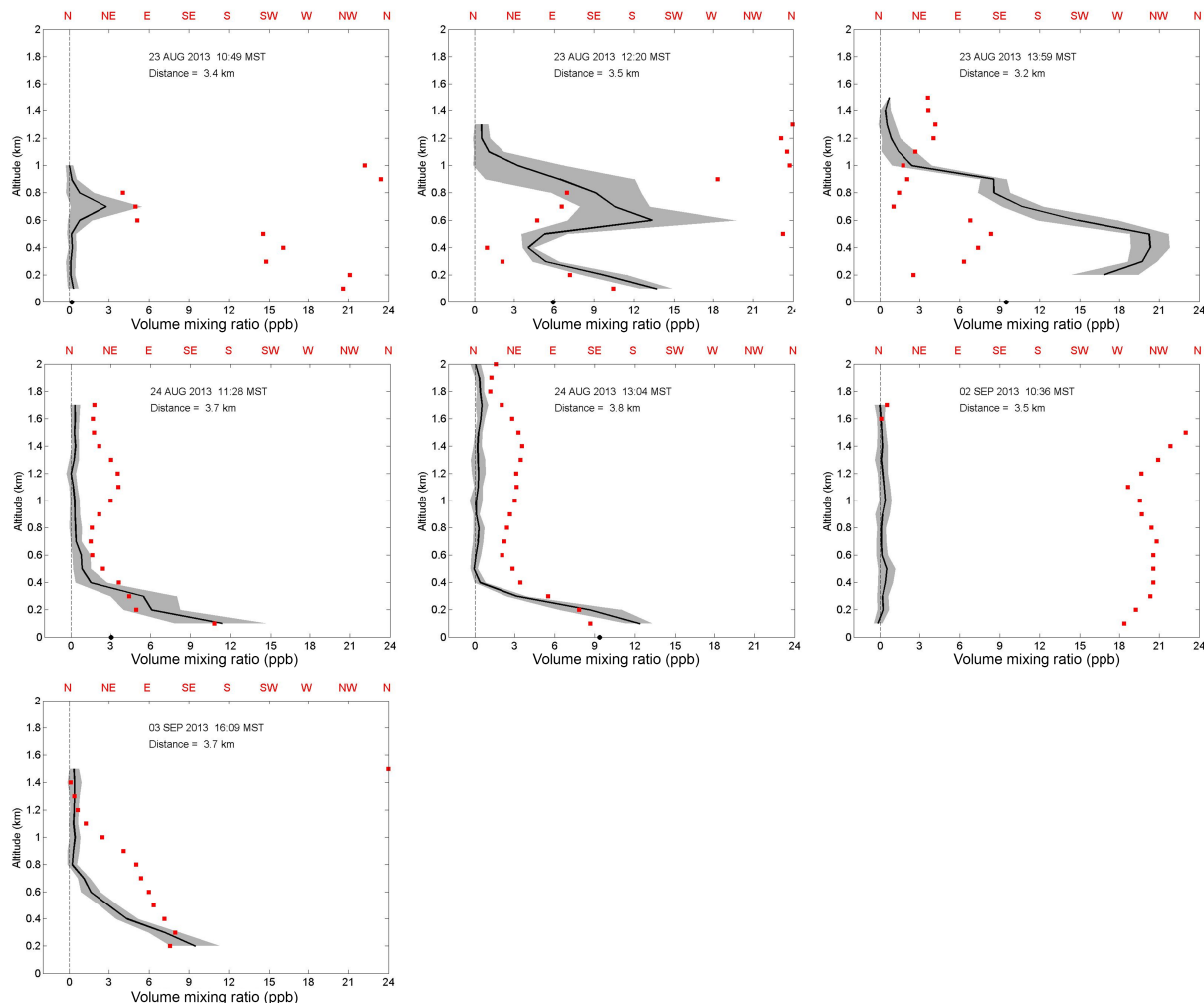
Aircraft-based measurements of air pollutants from sources in the Canadian oil sands were made in support of the Joint Canada–Alberta Implementation Plan for Oil Sands Monitoring during a summer intensive field campaign between 13 August and 7 September 2013 (Gordon et al., 2015). The SO_2 measurements from these flights were used to examine the accuracy of the Pandora VCDs. Specifically, seven spirals were flown within 4 km of Fort McKay in which vertical profiles were made with a Thermo Scientific 43iTLE analyser. The measured vertical profiles of SO_2 mixing ratios and the wind directions as a function of altitude for these seven flights are shown in Fig. 10. Integrated SO_2 columns were compared with Pandora VCDs, and the results are shown in Fig. 11 and Table 1. The minimum altitude range flown by the aircraft used to construct a profile was 100–1500 m, with most profiles exceeding 2000 m. The integrals were calculated for three scenarios for SO_2 concentrations below the lowest aircraft flight altitude of about 100–150 m: (1) assuming a zero mixing ratio between the ground and the lowest aircraft altitude, (2) assuming that the mixing ratio was constant as at the lowest aircraft altitude, and (3) with the mixing ratio linearly extrapolated below the lowest aircraft altitude. For most spirals an SO_2 value from the sur-

face was available to “anchor” the profile, and it was found to be consistent with the constant mixing ratio scenario. In five flights, the integrated SO_2 was very close to the Pandora values with differences within 0.25 DU. The Pandora instrument was able to track the increase in VCD spanning three spirals, capturing the onset on 23 August 2013 of a large pollution event. On two occasions where the aircraft measurements showed near-zero SO_2 concentrations, Pandora’s values were 0.12 DU and –0.2 DU, i.e. within the 1σ uncertainties of the measurements. Only for the final spiral was the aircraft VCD lower than the Pandora value by more than 0.5 DU. On that flight, both aircraft and Pandora data demonstrated elevated SO_2 values. The aircraft data showed a thin layer of SO_2 below 600 m with a maximum at 200 m (Fig. 10). That may be an indication of the edge of the plume, and the plume could be thicker along the Pandora optical path. Nevertheless, the average difference between the integrated aircraft values and Pandora VCDs was about 0.1 DU, with standard deviations of 0.37 or 0.29 DU if the last flight was excluded.

The Pandora SO_2 VCDs were also compared with measurements from the Dutch–Finnish Ozone Monitoring Instrument (OMI) on board NASA Aura satellite (Levelt et al., 2006). The recent version of the operational OMI SO_2 data set, based on the principal component analysis algorithm (Li et al., 2013) with additional adjustment based on modelled SO_2 profiles over the oil sands region (McLinden et al., 2014), was used in this comparison. We also limited the comparison to pixel sizes less than 40 km (track positions 11–50)

Table 1. SO_2 VCD calculated from measurements of seven aircraft flights, from Pandora 104 measurements and surface SO_2 concentrations.

Date and time (MST)	Min. aircraft VCD (DU)	Max. aircraft VCD (DU)	Pandora VCD (DU)	Surface (ppbv)
23 Aug 2013 10:49	0.04	0.04	0.16	0.16
23 Aug 2013 12:20	0.63	0.88	0.38	5.93
23 Aug 2013 13:59	1.08	1.31	1.10	9.49
24 Aug 2013 11:28	0.18	0.41	0.27	3.04
24 Aug 2013 13:04	0.15	0.39	0.72	9.36
02 Sep 2013 10:36	0.02	0.02	-0.21	
03 Sep 2013 16:09	0.26	0.51	1.06	

**Figure 10.** The measured vertical profiles of SO_2 mixing ratios in ppbv (the black lines) with 1σ uncertainties as a function of altitude for seven spiral flights around Fort McKay in August–September 2013. The black dots indicate mixing ratios at the surface. The red dots represent the wind directions as labelled on the top axis. Note that the two major SO_2 sources are located to the south and south–south east of Fort McKay. The dates and times of the flights and the mean distances from Fort McKay are also shown.

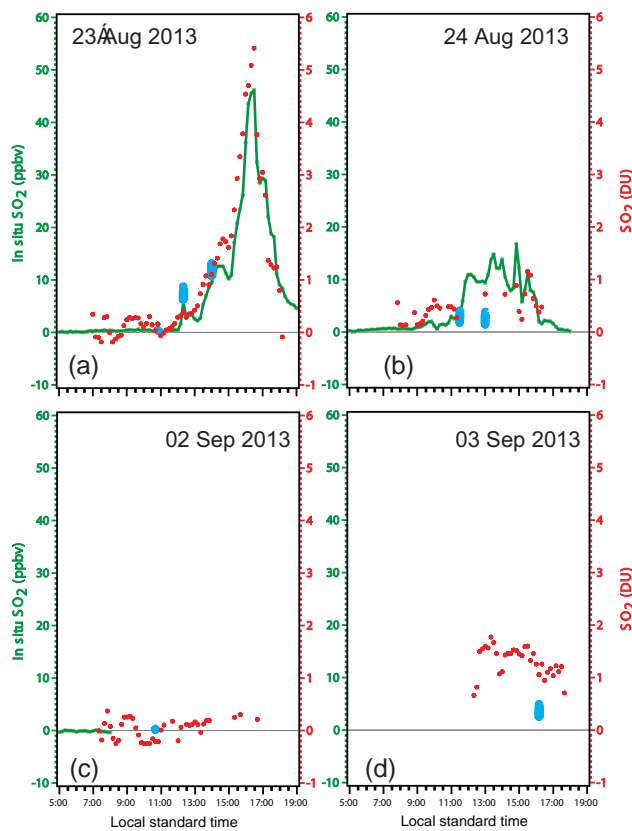


Figure 11. SO_2 VCD (DU) measured by the Pandora spectrometer (red) at Fort McKay and calculated from integrated aircraft SO_2 profile measurements (blue), as well as in situ SO_2 concentration in ppbv (green). The vertical blue bars represent the range of SO_2 VCDs calculated from two assumptions: for 0 mixing below the lowest aircraft flight height and a constant mixing ratio that corresponds to the mixing ratio at the lowest altitude where SO_2 was measured.

centred within 15 km from Fort McKay. Only OMI measurements taken under snow-free and cloud-free (cloud fraction <0.2) conditions were used. The Pandora values were averaged within ± 0.5 h from the OMI overpass time. A scatter plot of all 51 coincident OMI and Pandora measurements that satisfy these criteria is shown in Fig. 12. The correlation coefficient between the two data sets is only about 0.2 and this is not surprising given a large pixel size and high uncertainties of OMI measurements (0.5 DU at 1σ level) relative to the range of SO_2 levels. We simulated OMI and Pandora measurements using the EC GEM- MACH (Global Environmental Multi-scale – Modelling Air quality and Chemistry) (Makar et al., 2015a, b) model at 2.5 km resolution, accounting for the size of the OMI pixel and the 15 km coincidence criteria, and considering the addition of realistic measurement noise. A detailed discussion of this simulation is beyond the scope of this study, but we found that the correlation coefficient between such simulated Pandora and OMI data was only about 0.3. The model study indicates that the

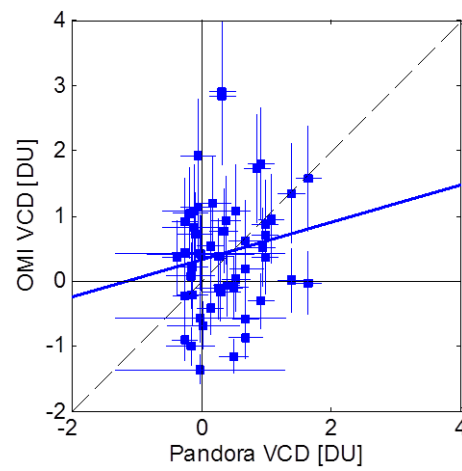


Figure 12. A scatter plot of SO_2 VCD values measured by the OMI satellite instrument and Pandora. The correlation coefficient between the two data sets is 0.17 and the slope of the regression line is 0.23. The error bars represent 2σ intervals.

main culprits in the degradation of the correlation were the measurement noise (primarily in the OMI) and the OMI horizontal resolution. This example demonstrates that a simple scatter plot comparison of satellite and ground-based VCD measurements is not very informative, and a proper account for satellite viewing geometry and measurement uncertainties is necessary.

5 Summary and discussion

In order to study variability and changes of VCDs of major pollutants such as SO_2 in the Canadian oil sands region, a Pandora sun photometer was installed at Fort McKay in August 2013. We found that the instrument is suitable for SO_2 monitoring and reliable enough to operate in remote areas. Originally, the instrument was deployed in a configuration with the instrument head mounted on a tripod and the spectrometer and computer installed in waterproof plastic housing. In August 2014, the instrument spectrometer was redeployed with the spectrometer and computer installed indoors in a temperature-controlled environment and the instrument optical head connected by an optical cable, located on the roof of the instrument trailer. In this modified configuration, the instrument demonstrated that it can operate for extended periods under cold conditions.

The instrument is sensitive enough to measure anthropogenic SO_2 from two major SO_2 sources, with total emissions of about 45 kt yr^{-1} , located approximately 20 km from the observation site. As expected, elevated VCD (up to 9 DU) and surface concentrations of SO_2 are observed when the wind is from the south and south-east, where the emission sources are located. With no industrial sources located to

the west, VCD and surface concentrations are about zero for westerly winds.

The calibration procedure applied in this study was similar to that developed by Herman et al. (2009) for NO_2 , but it was modified to account for a much higher noise level of SO_2 VCD measurements (0.01 DU for NO_2 vs. 0.17 DU for SO_2). This calibration procedure is based on the 25th (or 10th) percentile and makes the assumption that a sizable fraction of all measurements corresponds to SO_2 -free conditions. Fort McKay measurements stratified by the wind direction confirmed the validity of this approach: the average SO_2 values after the calibration procedure were close to zero for winds from the west where no SO_2 sources are found. This 25th (or 10th) percentile-based calibration approach is optimal when clean conditions occur frequently, e.g. for sites located in a vicinity of emission point sources where SO_2 VCDs depend on the wind direction. However, lower percentiles such as the 10th or smaller may be required in regions with persistent high SO_2 values, e.g. in eastern China.

Various sources of measurement uncertainties were examined. The statistical standard error of SO_2 VCD calculated by the spectral fitting algorithm is under 0.05 DU for 60 % and under 0.15 DU for 90 % of all direct-sun observations. The instrument precision, calculated from parallel measurements by two instruments, is about 0.17 DU (1σ). The spectral fitting procedure and the accuracy of the retrieved SO_2 values largely depend on properly accounting for ozone absorption and the reference spectrum. Based on some examples, we estimate that these factors can introduce errors up to 0.4 DU. Further development of the retrieval algorithms could improve the instrument accuracy. Measurements at Fort McKay, when the wind was from clean sectors, demonstrated that the overall Pandora uncertainty is under 0.26 DU (1σ). The Pandora measurements were further validated using seven aircraft profile measurements that demonstrated a bias within 0.1 DU and the standard deviation of the difference under 0.3 DU for all but one of the aircraft profiles.

When used for satellite validation, simple scatter plot comparisons of coincident satellite and ground-based VCD measurements are less informative for a localized industrial source such as the oil sands, and their interpretation requires a proper accounting of satellite viewing geometry and measurement uncertainties. The comparison of Pandora and OMI VCDs over Fort McKay demonstrated a low correlation, with a correlation coefficient of about 0.2. This is not surprising given a large pixel size, high uncertainties of OMI measurements (0.5 DU at 1σ level) relative to the range of SO_2 variations, and heterogeneity of the SO_2 spatial distribution at this location. The use of models to account for the difference in spatial and temporal resolution between ground-based and satellite measurements would greatly facilitate satellite SO_2 VCDs validation.

The comparison of SO_2 VCDs and surface concentrations at Fort McKay suggests that there is no simple link between these two quantities. High surface concentrations contribute to the column values. A simple statistical relationship suggests that, on average, each 10 ppbv of surface concentration roughly corresponds to 1 DU of total column (similar to what one would calculate for 10 ppbv spread through a 1 km surface layer). However, elevated VCDs may be related to plumes that are above the ground with little or no fumigation, and therefore may not produce elevated surface concentrations.

6 Data availability

Data from Pandora instruments are available through Environment and Climate Change Canada (contact Dr. Vitali Fioletov, vitali.fioletov@canada.ca). The data will also be available from a centralized Pandora data archive when such an archive is established.

Appendix A

Information about the natural variability of measured parameter and measurement uncertainties can be derived from the measurements themselves. This approach, also known as the Grubbs estimation method (Grubbs, 1948; Toohey and Strong, 2007), is often used to estimate the precision of measurements. For readers' convenience, we present the method here as it was described by Fioletov et al. (2006).

The result of a measurement (M) is the sum of the true measured value (X) and an error (e). Let us consider two instruments that measure the same parameter X , but with different errors e_1 and e_2 . The results of their measurements (M_1 and M_2) can be used to estimate the variances of X , e_1 , and e_2 , as follows. If we assume that the measured value and the errors are independent, then the variance of M is the sum of variances of X and e_i :

$$\sigma^2(M_i) = \sigma^2(X) + \sigma^2(e_i), i = 1, 2. \quad (\text{A1})$$

The difference of M_1 and M_2 does not depend on X . If, in addition, we assume that the errors of different instruments are not correlated, then the variance of the difference is equal to the sum of $\sigma^2(e_1)$ and $\sigma^2(e_2)$:

$$\sigma^2(M_1 - M_2) = \sigma^2(e_1) + \sigma^2(e_2). \quad (\text{A2})$$

The values of $\sigma^2(M_1)$, $\sigma^2(M_2)$, and $\sigma^2(M_1 - M_2)$ can be estimated from a set of parallel measurements. The three resulting equations can be solved for $\sigma^2(X)$, $\sigma^2(e_1)$, and $\sigma^2(e_2)$:

$$\sigma^2(X) = 1/2(\sigma^2(M_1) + \sigma^2(M_2) - \sigma^2(M_1 - M_2)), \quad (\text{A3})$$

$$\sigma^2(e_1) = 1/2(\sigma^2(M_1) - \sigma^2(M_2) + \sigma^2(M_1 - M_2)), \quad (\text{A4})$$

$$\sigma^2(e_2) = 1/2(\sigma^2(M_2) - \sigma^2(M_1) + \sigma^2(M_1 - M_2)). \quad (\text{A5})$$

Equation (3) was used to estimate the standard deviation (SD) of instrument errors (we will refer to it as to standard instrument uncertainty) and the SD of variability.

In reality, we do not actually know the variances $\sigma^2(M_i)$ and $\sigma^2(M_1 - M_2)$; we can only estimate them, with a certain error, from the available measurements. The α -level confidence interval for the variance σ^2 depends on the estimated variance value itself and the number of data points, n :

$$\frac{(n-1)s^2}{\chi^2_{1-\alpha/2}(n-1)} < \sigma^2 < \frac{(n-1)s^2}{\chi^2_{\alpha/2}(n-1)}, \quad (\text{A6})$$

where s^2 is the sample variance and $\chi^2(n-1)$ is the chi-square distribution with $n-1$ degrees of freedom. The error of the variance estimate depends on the variance itself. All three variances, $\sigma^2(M_1)$, $\sigma^2(M_2)$, and $\sigma^2(M_1 - M_2)$, determine $\sigma^2(X)$, $\sigma^2(e_1)$, and $\sigma^2(e_2)$ in Eq. (3). Therefore, the errors in the $\sigma^2(X)$, $\sigma^2(e_1)$, and $\sigma^2(e_2)$ estimates depend on the sum of all three variances $\sigma^2(M_1)$, $\sigma^2(M_2)$, and $\sigma^2(M_1 - M_2)$, and can be high even if the estimated variance itself is low (but one or more of the variances $\sigma^2(M_1)$, $\sigma^2(M_2)$, or $\sigma^2(M_1 - M_2)$ are high). The estimates are thus only as accurate as the least accurate of these parameters. The variance estimates can be improved by increasing the number of data points.

Acknowledgements. The authors wish to thank the NRC-FRL flight crew of the Convair 580 for making the airborne study possible. Funding for the airborne study over the oil sands region was provided in part by Environment Canada's Clean Air Regulatory Agenda (CARA). We acknowledge the NASA Earth Science Division for funding of OMI SO_2 product development and analysis. The Dutch-Finnish-built OMI instrument is part of the NASA's EOS Aura satellite payload. We thank systems engineering, instrument calibration, and satellite integration teams for making this mission a success. The OMI project is managed by KNMI and the Netherlands Space Agency (NSO).

Edited by: M. Weber

References

- Bais, A. F., Zerefos, C. S., Meleti, C., Ziomas, I. C., and Tourpali, K.: Spectral measurements of solar UVB radiation and its relation to total ozone, SO_2 , and clouds, *J. Geophys. Res.*, 98, 5199–5204, 1993.
- Carn, S. A., Krueger, A. J., Bluth, G. S. J., Schaefer, S. J., Krotkov, N. A., Watson, I. M., and Datta, S.: Volcanic eruption detection by the Total Ozone Mapping Spectrometer (TOMS) instruments: A 22-year record of sulfur dioxide and ash emissions, in: *Volcanic Degassing*, Special Publication of the Geological Society of London, edited by: Oppenheimer, C., Pyle, D. M., and Barclay, J., 177–202, Geological Society, London, UK, 2003.
- Carn, S. A., Krueger, A. J., Krotkov, N. A., Yang, K., and Levelt, P. F.: Sulfur dioxide emissions from Peruvian copper smelters detected by the Ozone Monitoring Instrument, *Geophys. Res. Lett.*, 34, L09801, doi:10.1029/2006GL029020, 2007.
- Carn, S. A., Krotkov, N. A., Yang, K., and Krueger, A. J.: Measuring global volcanic degassing with the Ozone Monitoring Instrument (OMI), *Geol. Soc. London, Spec. Publ.*, 380, 229–257, doi:10.1144/SP380.12, 2013.
- Clarisso, L., Fromm, M., Ngadi, Y., Emmons, L., Clerbaux, C., Hurtmans, D., and Coheur, P.-F.: Intercontinental transport of anthropogenic sulfur dioxide and other pollutants: An infrared remote sensing case study, *Geophys. Res. Lett.*, 38, L19806, doi:10.1029/2011GL048976, 2011.
- De Backer, H. and Muer, D. De: Intercomparison of total ozone data measured with Dobson and Brewer spectrophotometers at Uccle (Belgium) from January 1984 to March 1991, including zenith sky observations, *J. Geophys. Res.*, 96, 20711–20719, 1991.
- de Foy, B., Krotkov, N. A., Bei, N., Herndon, S. C., Huey, L. G., Martínez, A.-P., Ruiz-Suárez, L. G., Wood, E. C., Zavala, M., and Molina, L. T.: Hit from both sides: tracking industrial and volcanic plumes in Mexico City with surface measurements and OMI SO_2 retrievals during the MILAGRO field campaign, *Atmos. Chem. Phys.*, 9, 9599–9617, doi:10.5194/acp-9-9599-2009, 2009.
- Eisinger, M. and Burrows, J. P.: Tropospheric sulfur dioxide observed by the ERS-2 GOME instrument, *Geophys. Res. Lett.*, 25, 4177–4180, 1998.
- Fiioletov, V. E., Griffioen, E., Kerr, J. B., Wardle, D. I., and Uchino, O.: Influence of volcanic sulfur dioxide on spectral UV irradiance as measured by Brewer Spectrophotometers, *Geophys. Res. Lett.*, 25, 1665–1668, doi:10.1029/98GL51305, 1998.
- Fiioletov, V. E., Tarasick, D. W., and Petropavlovskikh, I.: Estimating ozone variability and instrument uncertainties from SBUV(2), ozonesonde, Umkehr, and SAGE II measurements: Short-term variations, *J. Geophys. Res.*, 111, D02305, doi:10.1029/2005JD006340, 2006.
- Fiioletov, V. E., McLinden, C. A., Krotkov, N., Moran, M. D., and Yang, K.: Estimation of SO_2 emissions using OMI retrievals, *Geophys. Res. Lett.*, 38, L21811, doi:10.1029/2011GL049402, 2011.
- Fiioletov, V. E., McLinden, C. A., Krotkov, N., Yang, K., Loyola, D. G., Valks, P., Theys, N., Van Roozendael, M., Nowlan, C. R., Chance, K., Liu, X., Lee, C., and Martin, R. V.: Application of OMI, SCIAMACHY, and GOME-2 satellite SO_2 retrievals for detection of large emission sources, *J. Geophys. Res.-Atmos.*, 118, 11399–11418, doi:10.1002/jgrd.50826, 2013.
- Galle, B., Johansson, M., Rivera, C., Zhang, Y., Kihlman, M., Kern, C., Lehmann, T., Platt, U., Arellano, S., and Hidalgo, S.: Network for Observation of Volcanic and Atmospheric Change (NOVAC) – A global network for volcanic gas monitoring: Network layout and instrument description, *J. Geophys. Res.*, 115, D05304, doi:10.1029/2009JD011823, 2010.
- Georgoulias, A. K., Balis, D., Koukouli, M. E., Meleti, C., Bais, A., and Zerefos, C.: A study of the total atmospheric sulfur dioxide load using ground-based measurements and the satellite derived Sulfur Dioxide Index, *Atmos. Environ.*, 43, 1693–1701, doi:10.1016/j.atmosenv.2008.12.012, 2009.
- Gordon, M., Li, S.-M., Staebler, R., Darlington, A., Hayden, K., O'Brien, J., and Wolde, M.: Determining air pollutant emission rates based on mass balance using airborne measurement data over the Alberta oil sands operations, *Atmos. Meas. Tech.*, 8, 3745–3765, doi:10.5194/amt-8-3745-2015, 2015.
- Grubbs, F. E.: On estimating precision of measuring instruments and product variability, *J. Am. Stat. Assoc.*, 42, 243–264, 1948.
- Herman, J., Cede, A., Spinei, E., Mount, G., Tzortziou, M., and Abu Hassan, N.: NO_2 column amounts from ground-based Pandora and MFDOAS spectrometers using the direct-sun DOAS technique: Intercomparisons and application to OMI validation, *J. Geophys. Res.*, 114, D13307, doi:10.1029/2009JD011848, 2009.
- Herman, J., Evans, R., Cede, A., Abu Hassan, N., Petropavlovskikh, I., and McConville, G.: Comparison of ozone retrievals from the Pandora spectrometer system and Dobson spectrophotometer in Boulder, Colorado, *Atmos. Meas. Tech.*, 8, 3407–3418, doi:10.5194/amt-8-3407-2015, 2015.
- Hutchinson, T. C. and Whitby, L. M.: The effects of acid rainfall and heavy metal particulates on a boreal Forest ecosystem near the Sudbury smelting region of Canada, *Water. Air. Soil Pollut.*, 7, 421–438, doi:10.1007/BF00285542, 1977.
- Kelly, E. N., Schindler, D. W., Hodson, P. V., Short, J. W., Radmanovich, R., and Nielsen, C. C.: Oil sands development contributes elements toxic at low concentrations to the Athabasca River and its tributaries, *P. Natl. Acad. Sci. USA*, 107, 16178–16183, doi:10.1073/pnas.1008754107, 2010.
- Kerr, J. B.: New methodology for deriving total ozone and other atmospheric variables from Brewer spectrophotometer direct sun spectra, *J. Geophys. Res.*, 107, 4731, doi:10.1029/2001JD001227, 2002.
- Kerr, J. B., Asbridge, I. A., and Evans, W. F. J.: Intercomparison of total ozone measured by the Brewer and Dobson spec-

- trophotometers at Toronto, *J. Geophys. Res.*, 93, 11129–11140, doi:10.1029/JD093iD09p11129, 1988.
- Knepp, T., Pippin, M., Crawford, J., Chen, G., Szykman, J., Long, R., Cowen, L., Cede, A., Abuhaman, N., Herman, J., Delgado, R., Compton, J., Berkoff, T., Fishman, J., Martins, D., Stauffer, R., Thompson, A. M., Weinheimer, A., Knapp, D., Montzka, D., Lenschow, D., and Neil, D.: Estimating surface NO_2 and SO_2 mixing ratios from fast-response total column observations and potential application to geostationary missions, *J. Atmos. Chem.*, 72, 261–286, doi:10.1007/s10874-013-9257-6, 2015.
- Koenker, R. and Bassett, G. W.: Regression Quantiles, *Econometrica*, 46, 33–50, 1978.
- Krotkov, N. A., McLinden, C. A., Li, C., Lamsal, L. N., Celarier, E. A., Marchenko, S. V., Swartz, W. H., Bucsela, E. J., Joiner, J., Duncan, B. N., Boersma, K. F., Veefkind, J. P., Levelt, P. F., Fioletov, V. E., Dickerson, R. R., He, H., Lu, Z., and Streets, D. G.: Aura OMI observations of regional SO_2 and NO_2 pollution changes from 2005 to 2015, *Atmos. Chem. Phys.*, 16, 4605–4629, doi:10.5194/acp-16-4605-2016, 2016.
- Krueger, A. J., Walter, L. S., Bhartia, P. K., Schnetzler, C. C., Krotkov, N. A., Sprod, I., and Bluth, G. J. S.: Volcanic sulfur dioxide measurements from the Total Ozone Mapping Spectrometer instruments, *J. Geophys. Res.*, 100, 14057–14076, doi:10.1029/95JD01222, 1995.
- Krueger, A. J., Schaefer, S. J., Krotkov, N., Bluth, G., and Barker, S.: Ultraviolet remote sensing of volcanic emissions, in: *Remote Sensing of Active Volcanism*, vol. 116, edited by: Mouginis, M. and Crisp, J., 25–43, American Geophysical Union, 2000.
- Lee, C., Martin, R. V., Van Donkelaar, A., Lee, H., Dickerson, R. R., Hains, J. C., Krotkov, N., Richter, A., Vinnikov, K., and Schwab, J. J.: SO_2 emissions and lifetimes: Estimates from inverse modeling using in situ and global, space-based (SCIAMACHY and OMI) observations, *J. Geophys. Res.*, 116, D06304, doi:10.1029/2010JD014758, 2011.
- Levelt, P. F., van den Oord, G. H. J., Dobber, M. R., Malkki, A., Stammes, P., Lundell, J. O. V., and Saari, H.: The Ozone Monitoring Instrument, *IEEE T. Geosci. Remote Sens.*, 44, 1093–1101, doi:10.1109/TGRS.2006.872333, 2006.
- Li, C., Joiner, J., Krotkov, N. A., and Bhartia, P. K.: A fast and sensitive new satellite SO_2 retrieval algorithm based on principal component analysis: Application to the ozone monitoring instrument, *Geophys. Res. Lett.*, 40, 6314–6318, doi:10.1002/2013GL058134, 2013.
- Longo, B. M., Yang, W., Green, J. B., Crosby, F. L., and Crosby, V. L.: Acute health effects associated with exposure to volcanic air pollution (vog) from increased activity at Kilauea Volcano in 2008, *J. Toxicol. Environ. Health. A*, 73, 1370–1381, doi:10.1080/15287394.2010.497440, 2010.
- Makar, P. A., Gong, W., Hogrefe, C., Zhang, Y., Curci, G., Zabkar, R., Milbrandt, J., Im, U., Balzarini, A., Baro, R., Bianconi, R., Cheung, P., Forkel, R., Gravel, S., Hirtl, H., Honzak, L., Hou, A., Jimenz-Guerrero, P., Langer, M., Moran, M. D., Pabla, B., Perez, J. L., Pirovano, G., San Jose, R., Tuccella, P., Werhahn, J., Zhang, J., and Galmarini, S.: Feedbacks between air pollution and weather, part 2: Effects on chemistry, *Atmos. Environ.*, 115, 499–526, doi:10.1016/j.atmosenv.2014.10.021, 2015a.
- Makar, P. A., Gong, W., Milbrandt, J., Hogrefe, C., Zhang, Y., Curci, G., Zabkar, R., Im, U., Balzarini, A., Baro, R., Bianconi, R., Cheung, P., Forkel, R., Gravel, S., Hirtl, H., Honzak, L., Hou, A., Jimenz-Guerrero, P., Langer, M., Moran, M. D., Pabla, B., Perez, J. L., Pirovano, G., San Jose, R., Tuccella, P., Werhahn, J., Zhang, J., and Galmarini, S.: Feedbacks between air pollution and weather, part 1: Effects on weather, *Atmos. Environ.*, 115, 442–469, doi:10.1016/j.atmosenv.2014.12.003, 2015b.
- McLinden, C. A., Fioletov, V., Boersma, K. F., Krotkov, N., Sioris, C. E., Veefkind, J. P., and Yang, K.: Air quality over the Canadian oil sands: A first assessment using satellite observations, *Geophys. Res. Lett.*, 39, 1–8, doi:10.1029/2011GL050273, 2012.
- McLinden, C. A., Fioletov, V., Boersma, K. F., Kharol, S. K., Krotkov, N., Lamsal, L., Makar, P. A., Martin, R. V., Veefkind, J. P., and Yang, K.: Improved satellite retrievals of NO_2 and SO_2 over the Canadian oil sands and comparisons with surface measurements, *Atmos. Chem. Phys.*, 14, 3637–3656, doi:10.5194/acp-14-3637-2014, 2014.
- McLinden, C., Fioletov, V., Krotkov, N. A., Li, C., Boersma, K. F., and Adams, C.: A decade of change in NO_2 and SO_2 over the Canadian oil sands as seen from space, *Environ. Sci. Technol.*, 50, 331–337, doi:10.1021/acs.est.5b04985, 2015.
- Nowlan, C. R., Liu, X., Chance, K., Cai, Z., Kurosu, T. P., Lee, C., and Martin, R. V.: Retrievals of sulfur dioxide from the Global Ozone Monitoring Experiment 2 (GOME-2) using an optimal estimation approach: Algorithm and initial validation, *J. Geophys. Res.*, 116, D18301, doi:10.1029/2011JD015808, 2011.
- Platt, U. and Stutz, J.: Differential Optical Absorption Spectroscopy, Springer, Berlin, Heidelberg, 2008.
- Pope, C. A. and Dockery, D. W.: Health effects of fine particulate air pollution: Lines that connect, *J. Air Waste Manag. Assoc.*, 56, 709–742, 2006.
- Reed, A. J., Thompson, A. M., Kollonige, D. E., Martins, D. K., Tzortziou, M. A., Herman, J. R., Berkoff, T. A., Abuhaman, N. K., and Cede, A.: Effects of local meteorology and aerosols on ozone and nitrogen dioxide retrievals from OMI and pandora spectrometers in Maryland, USA during DISCOVER-AQ 2011, *J. Atmos. Chem.*, 72, 455–482, doi:10.1007/s10874-013-9254-9, 2013.
- Richter, A., Weber, M., Burrows, J. P., Lambert, J.-C., and van Gijsel, A.: Validation strategy for satellite observations of tropospheric reactive gases, *Ann. Geophys.*, 56, 1–10, doi:10.4401/ag-6335, 2013.
- Rix, M., Valks, P., Hao, N., Loyola, D., Schlager, H., Huntrieser, H., Flemming, J., Koehler, U., Schumann, U., and Inness, A.: Volcanic SO_2 , BrO and plume height estimations using GOME-2 satellite measurements during the eruption of Eyjafjallajökull in May 2010, *J. Geophys. Res.-Atmos.*, 117, D00U19, doi:10.1029/2011JD016718, 2012.
- Simpson, I. J., Blake, N. J., Barletta, B., Diskin, G. S., Fuelberg, H. E., Gorham, K., Huey, L. G., Meinardi, S., Rowland, F. S., Vay, S. A., Weinheimer, A. J., Yang, M., and Blake, D. R.: Characterization of trace gases measured over Alberta oil sands mining operations: 76 speciated $\text{C}_2\text{-}\text{C}_{10}$ volatile organic compounds (VOCs), CO_2 , CH_4 , CO , NO , NO_2 , NO_y , O_3 and SO_2 , *Atmos. Chem. Phys.*, 10, 11931–11954, doi:10.5194/acp-10-11931-2010, 2010.
- Theys, N., Campion, R., Clarisse, L., Brenot, H., van Gent, J., Dils, B., Corradini, S., Merucci, L., Coheur, P.-F., Van Roozendael, M., Hurtmans, D., Clerbaux, C., Tait, S., and Ferrucci, F.: Volcanic SO_2 fluxes derived from satellite data: a survey using OMI, GOME-2, IASI and MODIS, *Atmos. Chem. Phys.*, 13, 5945–5968, doi:10.5194/acp-13-5945-2013, 2013.

- Theys, N., Smedt, I. De, Gent, J. Van, Danckaert, T., Wang, T., Hendrick, F., Stavrakou, T., Bauduin, S., Clarisse, L., Li, C., Krotkov, N., Yu, H., Brenot, H., and Roozendael, M. Van: Sulfur dioxide vertical column DOAS retrievals from the Ozone Monitoring Instrument: Global observations and comparison to ground-based and satellite data, *J. Geophys. Res.*, 120, 2470–2491, doi:10.1002/2014JD022657, 2015.
- Thomas, W., Erbertseder, T., Ruppert, T., Roozendael, M. Van, Verdebout, J., Balis, D., Meleti, C., and Zerefos, C.: On the retrieval of volcanic sulfur dioxide emissions from GOME backscatter measurements, *J. Atmos. Chem.*, 50, 295–320, doi:10.1007/s10874-005-5544-1, 2005.
- Toohey, M. and Strong, K.: Estimating biases and error variances through the comparison of coincident satellite measurements, *J. Geophys. Res.-Atmos.*, 112, 1–12, D13306, doi:10.1029/2006jd008192, 2007.
- Tzortziou, M., Herman, J. R., Cede, A., and Abuhassan, N.: High precision, absolute total column ozone measurements from the Pandora spectrometer system: Comparisons with data from a Brewer double monochromator and Aura OMI, *J. Geophys. Res.*, 117, D16303, doi:10.1029/2012JD017814, 2012.
- Tzortziou, M., Herman, J. R., Cede, A., Loughner, C. P., Abuhassan, N., and Naik, S.: Spatial and temporal variability of ozone and nitrogen dioxide over a major urban estuarine ecosystem, *J. Atmos. Chem.*, 72, 287–309, doi:10.1007/s10874-013-9255-8, 2013.
- Vandaele, A. C., Simon, P. C., Guilmot, J. M., Carleer, M., and Colin, R.: SO_2 absorption cross section measurement in the UV using a Fourier transform spectrometer, *J. Geophys. Res.*, 99, 25599–25605, 1994.
- Wang, T., Hendrick, F., Wang, P., Tang, G., Clémer, K., Yu, H., Fayt, C., Hermans, C., Gielen, C., Müller, J.-F., Pinardi, G., Theys, N., Brenot, H., and Van Roozendael, M.: Evaluation of tropospheric SO_2 retrieved from MAX-DOAS measurements in Xianghe, China, *Atmos. Chem. Phys.*, 14, 11149–11164, doi:10.5194/acp-14-11149-2014, 2014.
- Wood, J.: Environmental Policy Indicators – Air Quality, Studies in Environmental Policy, Fraser Institute., 2012.
- Wu, F. C., Xie, P. H., Li, A., Chan, K. L., Hartl, A., Wang, Y., Si, F. Q., Zeng, Y., Qin, M., Xu, J., Liu, J. G., Liu, W. Q., and Wenig, M.: Observations of SO_2 and NO_2 by mobile DOAS in the Guangzhou eastern area during the Asian Games 2010, *Atmos. Meas. Tech.*, 6, 2277–2292, doi:10.5194/amt-6-2277-2013, 2013.
- Zerefos, C., Ganev, K., Kourtidis, K., Tzortziou, M., Vasaras, A., and Syrakov, E.: On the origin of SO_2 above Northern Greece, *Geophys. Res. Lett.*, 27, 365–368, doi:10.1029/1999GL010799, 2000.